

Mincle signaling exacerbates acetaminophen-induced liver injury by promoting Kupffer cell activation in mice

Authors:

Jing Zhao^{1,3}, Jong-Won Kim¹, Zixiong Zhou¹, Jing Qi¹, Weishun Tian¹, Chae Woong Lim¹, Kang Min Han^{2*}, Bumseok Kim^{1*}

Author Affiliations:

1. Biosafety Research Institute and College of Veterinary Medicine, Jeonbuk National University, Iksan, Jeonbuk, Republic of Korea
2. Department of Pathology, Dongguk University Ilsan Hospital, Goyang, Republic of Korea
3. College of Animal Science and Technology, Henan University of Science and Technology, Luoyang, Henan, People's Republic of China

Running Title: Mincle signaling exacerbates APAP-induced liver injury

***Corresponding Author:**

Bumseok Kim, DVM, Ph.D.

College of Veterinary Medicine, Jeonbuk National University.

Iksan, Republic of Korea, 54531

Email: bskims@jbnu.ac.kr

Tel. No: (82)-63-850-0953

Fax No: (82)-63-850-0980

Kang Min Han, MD, Ph.D.

Department of Pathology, Dongguk University Ilsan Hospital,

Goyang, Republic of Korea, 10326

Email: kiekie53@hanmail.net

Tel. No: (82)-31-961-7932

Fax No: (82)-31-961-7939

Number of pages: 31

Number of tables: 1

Number of figures: 9

Number of References: 48

Number of words in Abstract: 250

Number of words in Introduction: 850

Number of words in Discussion: 838

Abbreviations:

APAP, acetaminophen; CYP, cytochrome P-450; DAMPs, danger-associated molecular patterns; DC, dendritic cells; GdCl₃, gadolinium chloride hexahydrate; KC, Kupffer cell, Mincle, macrophage-inducible C-type lectin; MPO, myeloperoxidase; NAPQI, N-acetyl-p-benzoquinone imine; NLRP3, nucleotide-binding domain and leucine-rich repeat protein 3; NPCs, non-parenchymal cells; PAMPs, pathogen-associated molecular patterns; SAP130, spliceosome associated protein 130; TDB, trehalose-6,6-dibehenate.

Abstract

Overdose of acetaminophen (APAP) has become one of the most reasons to induce acute liver failure. Macrophage-inducible C-type lectin (Mincle) acts as a key moderator in immune responses by recognizing spliceosome associated protein 130 (SAP130), which is an endogenous ligand released by necrotic cells. This study aims to explore the function of Mincle in APAP-induced hepatotoxicity. Wild-type (WT) and Mincle knockout (KO) mice were used to induce acute liver injury by injection of APAP. The hepatic expressions of Mincle, SAP130, and Mincle signaling intermediate (Syk) were markedly up-regulated following the APAP challenge. Mincle KO mice showed attenuated injury in the liver, as shown by reduced pathological lesions, decreased ALT and AST levels, down-regulated levels of inflammatory cytokines, and decreased neutrophil infiltration. Consistently, inhibition of Syk signaling by GS9973 alleviated APAP hepatotoxicity. Most importantly, Kupffer cells (KCs) were found as the major cellular source of Mincle. The depletion of KCs abolished the detrimental role of Mincle, and the adoptive transfer of WT KC to Mincle KO mice partially reversed the hyporesponsiveness to hepatotoxicity induced by APAP. Furthermore, the expression levels of interleukin (IL)-1 β and neutrophil-attractant CXC chemokines were substantially lower in KCs isolated from APAP-treated Mincle KO mice compared with those from WT mice. Similar results were found in primary Mincle KO KCs treated with a ligand of Mincle (trehalose-6, 6-dibehenate, TDB) or in conditioned media obtained from APAP-treated hepatocytes. Collectively, Mincle can regulate the inflammatory response of KCs, which is necessary for the complete progression of hepatotoxicity induced by APAP.

Significance statement

Acetaminophen (APAP) overdose is becoming a main reason to induce drug-induced acute liver damage in the developed world. This study showed that macrophage-inducible C-type lectin (Mincle) deletion or inhibition of Mincle downstream signaling attenuate APAP hepatotoxicity. Furthermore, Mincle as a modulator of Kupffer cell activation contributes to the full process of hepatotoxicity induced by APAP. This mechanism will offer valuable insights to overcome the limitation of APAP hepatotoxicity treatment.

Introduction

As a widely used analgesic and antipyretic drug, acetaminophen (APAP) has an excellent safety profile at therapeutic doses. However, acute or accumulated excessive APAP can evoke severe liver damage, resulting in acute liver failure (Chun et al., 2009; Jaeschke and Bajt, 2006). Epidemiological research showed that half of the patients with APAP overdoses were cases of unintentional overdosing when more than one APAP-containing analgesic were taken (Larson et al., 2005). Recently, programmed necrosis has been better termed as cell death mode induced by APAP (Jaeschke et al., 2019). APAP hepatotoxicity is triggered by N-acetyl-p-benzoquinone imine (NAPQI), which is a reactive metabolite of cytochrome P-450 (CYP) isoenzyme, especially CYP2E1 (Zaher et al., 1998; Chen et al., 2020). The toxicity of NAPQI is relieved by binding to hepatic glutathione (GSH). Once GSH is exhausted, excessive NAPQI eventually leads to mitochondrial oxidative stress and hepatocellular necrosis through binding to mitochondrial proteins (Larsen and Wendon, 2014). Based on the insights into this mechanism knowledge, the drug N-acetylcysteine (NAC), which is used in the synthesis of GSH, has been introduced to treat the patients suffering from APAP hepatotoxicity (Prescott et al., 1977). In particular, the benefit of NAC is better when it is administered at the earliest after taking overdose of APAP (Smilkstein et al., 1988; Lancaster et al., 2015).

Hepatocellular necrosis causes the secretion of various danger-associated molecular patterns (DAMPs) including histones, high mobility group box 1 (HMGB1) and DNA. DAMPs are host biomolecules that can be recognized by non-parenchymal cells (NPCs), especially resident hepatic Kupffer cells (KCs), resulting in the activation of NPCs in an autocrine manner (Martin-Murphy et al., 2010). The formation of the inflammasome by KCs then activates the innate immune system, causing substantial infiltration of neutrophils and macrophages to the inflammation site (Lawson et al., 2000; Holt et al., 2008). The systemic inflammation along with consequently advancing hepatocellular necrosis causes acute liver

failure leading to mortality.

As one of the C-type lectin superfamily members, macrophage-inducible C-type lectin, also called Mincle, is found to be detected on myeloid cells such as macrophages, neutrophils, and dendritic cells (DCs). Mincle signaling is necessary for the formation of the innate immune system, and in particular, it was found to be strongly induced when stimulated by inflammatory materials (Matsumoto et al., 1999; Richardson and Williams, 2014). As a transmembrane receptor, Mincle has an extracellular carbohydrate-recognition domain, which mediates interaction with ITAM-bearing adaptor molecule Fc receptor γ -chain (FcR γ) (Yamasaki et al., 2008). Furthermore, Mincle is activated by the mycobacterial cell wall component, trehalose-6,6-dimycolate (TDM), and the synthetic analog trehalose-6,6-dibehenate (TDB) (Ishikawa et al., 2009; Lin et al., 2017). Additionally, activation of Mincle can be induced by a release of small nuclear ribonucleoprotein component called spliceosome-associated protein130 (SAP130) (Brown, 2008; Yamasaki et al., 2008). Mincle signaling induces inflammatory responses through the recruited CARD9 adaptor protein and phosphorylated Syk, leading to inflammatory responses with the generation of cytokines including TNF- α and IL-6 (Brown, 2008).

Recently, a large amount of evidence has indicated that the Mincle signaling pathway plays an important role in noninfectious inflammatory disorders (de Rivero Vaccari et al., 2015; He et al., 2015). Moreover, studies have revealed that Mincle deletion protects against ethanol or concanavalin A-induced liver injury (Kim et al., 2018; Zhou et al., 2016; Greco et al., 2016). Currently, the effects of Mincle signaling on APAP hepatotoxicity have not been completely explored yet. Therefore, we investigated the role of Mincle in the progression of APAP hepatotoxicity and investigated the underlying mechanism.

Materials and methods

Experimental mice and protocol

Wild-type (WT) male C57BL/6N mice (8-week) were obtained from Taconic Farms, Inc. (Samtako Bio Korea, O-San, Republic of Korea). Mincle knockout (KO) mice were kindly provided by Professor Young-Joon Kim (Yonsei University, Republic of Korea) and backcrossed on C57BL/6N mice for at least ten generations (Lee et al., 2012). Mice were kept in a standard condition ($24 \pm 2^\circ\text{C}$, $50 \pm 5\%$ humidity, 12 h light/dark cycle). Animal management procedures and breeding facilities have been approved by the requirements of the Animal Care and Ethics Committees of Jeonbuk National University.

To induce liver injury, animals were fasted for 16 h and intraperitoneally (i.p.) injected indicated dose of APAP (150-500 mg/kg) (Sigma- Aldrich, St Louis, MO). In the selected experiments, mice were pretreated with an oral administration of a Syk inhibitor, entospletinib (GS-9973; Cayman Chemical, Ann Arbor, MI) (Currie et al., 2014) or vehicle control 1 h before APAP injection. To reveal the role of macrophages in APAP-induced liver injury, gadolinium chloride hexahydrate (GdCl_3 ; Sigma-Aldrich) was administered intravenously to mice (10 mg/kg) to inhibit or deplete the KCs (Merlin et al., 2016; Chatterjee et al., 2013). Subsequently, mice were anesthetized after 24 h of APAP injection, and blood was collected by cardiac puncture. Sizes of the tested animal groups in different experiments were chosen according to standard guidelines (Michel et al., 2020) and also dictated by the available number of mice of suitable strains, age and weight. Livers were harvested for gene expression and histological analysis.

Hepatocytes and KCs isolation

Primary hepatocytes from WT or Mincle KO mice were prepared by collagen perfusion. Briefly, collagenase 1 passing through the portal vein was used to digest mouse livers. The

digested cells were suspended and centrifuged at $50 \times g$ for 3 min. The pellet representing hepatocytes were collected and re-suspended after centrifugation, filtered, and washed several times. Cellular viability and cell number were measured by the Trypan blue dye exclusion method (Sigma-Aldrich).

Primary KCs were isolated from mice liver (Zhao et al., 2020). Briefly, the digested liver cells were centrifuged at $50 \times g$ for 3 min, and NPCs were collected from the supernatant. Then Percoll density gradient centrifugation was performed for the enrichment of KCs. KCs fractions were collected from the interface of 40% and 70% Percoll after centrifugation at $750 \times g$ for 20 min without brake. The positive selection of KCs was performed by magnetic cell sorting using the anti-F4/80 antibody (e-Biosciences, Cat# 13-4801-85).

Adoptive transfer of KCs

Macrophage adoptive transfer was performed as described previously (Chatterjee et al., 2013; Wu et al., 2012; Greco et al., 2016). Briefly, isolated F4/80⁺ KCs from WT mice were injected intravenously into macrophage depleted WT or Mincle KO recipients (1×10^6 cells per mouse in 200 μ L sterile PBS per injection). After 24 h, mice were injected with 300 mg/kg APAP.

Histopathologic and immunohistochemical examination

Mouse hepatic tissue was routinely fixed, processed, and embedded in paraffin wax. Tissue sections (5 μ m) were prepared. For histological analysis, hematoxylin and eosin (H&E) staining or terminal deoxynucleotidyl transferase-mediated dUTP nick-end labeling (TUNEL) staining were performed on tissue sections, and histological observation was done by light microscopy (BX-51, Olympus Corp., Tokyo, Japan). Positive areas of TUNEL-labeled cells

were determined on a computerized grid as described previously (Zhao et al., 2020). For immunohistochemical staining, tissue sections were stained with anti-mouse myeloperoxidase (MPO; Abcam, Cat# ab9535), which is a neutrophil marker, as described previously (Kim et al., 2018). Slide images were taken under a light microscope (BX-51; Olympus Corp.) in a blinded manner and subjected to digital image analysis (analySIS TS; Olympus Corp.).

Biochemical measurements

Commercial kits were used to measure the serum levels of alanine aminotransferase (ALT) and aspartate aminotransferase (AST) (ASAN Pharmaceutical, Hwasung, Republic of Korea). Samples of serum were prepared by centrifugation ($1000 \times g$, 15 min, 4°C). Hepatic GSH levels were measured by a GSH quantification kit (Dojindo, Kumamoto, Japan). An EMax spectrophotometer (Molecular Devices, Sunnyvale, CA) was used to determine the optical density at a wavelength of 490 or 412 nm.

Enzyme-linked immunosorbent assay (ELISA)

Protein extracted from the liver was used for quantification of the levels of cytokines. After centrifugation at $13,000 \times g$ for 15 min at 4°C , the precipitate was discarded and protein concentration in the supernatant was determined using the Pierce BCA Protein Assay kit (Thermo Fisher Scientific Inc.). The levels of each respective cytokines were determined using the commercial ELISA kits (eBioscience, San Diego, CA, USA). All experiments were performed according to the manufacturer's instructions.

Flow cytometric analysis

NPCs isolated from the liver were stained with Fc blocking reagent (BD Biosciences, Cat#

553142) for 20 min, followed by incubation with fluorescently conjugated anti-CD11b antibody (BD Biosciences, Cat# 550993) and anti-Ly6G antibody (e-Biosciences, Cat# 12-9668-82) on ice for 30 min. Each sample in experiments was performed by an Accuri C6 flow cytometer (BD Biosciences, Franklin Lakes, New Jersey, USA) and analyzed by BD CFlow®Plus software v. 1.0.227.4 (BD Biosciences, Franklin Lakes, New Jersey, USA). Target cell frequencies were expressed as the percentage for a specific cell subset.

LDH assay

Lactate dehydrogenase (LDH) assay was used to evaluate the hepatocellular cytotoxicity based on the measurement of the levels of LDH released into the culture medium with Cytotoxicity Detection Kit (Sigma-Aldrich). An EMax spectrophotometer (Molecular Devices, Sunnyvale, CA) was used to determine the optical density at a wavelength of 490 nm.

Quantitative real-time PCR (qPCR)

The Easy-Spin Total RNA extraction kit (GeneAll, Republic of Korea) was used to extract total RNA from liver tissue or cells. cDNA was prepared by treatment with gDNA remover, following with random primer and MultiScribe MuLV Reverse Transcriptase (Toyobo Co.). qPCR was performed on a CFX96 Real-Time PCR Detection System (Bio-Rad Laboratories, Hercules, CA) with cDNA. Glyceraldehyde-3-phosphate dehydrogenase (GAPDH) was used as an internal control to analyze the quantification. All PCR primers were purchased from Bioneer (Daejeon, Republic of Korea). PCR primer sequences are shown in Table 1. All experiments were performed according to the manufacturer's instructions.

Immunoblot analysis

Protein from liver tissues was lysed and measured concentration. After subjected protein to SDS-PAGE and transferred to polyvinylidene difluoride membrane, blocking was prepared with 5% bovine serum albumin in Tris-buffered saline containing 0.05% Tween-20 (TBS-T) for 1 h at room temperature. Subsequently, the following antibodies were used at a 1:1,000 dilution in a blocking buffer at 4°C overnight: anti-pSyk antibody (Cell Signaling Technology, Cat# 2710), anti-Syk antibody (Cell Signaling Technology, Cat# 2712), anti-SAP130 antibody (GeneTex Inc., Cat# GTX122554), anti-Mincle antibody (MBL International Corporation, Cat# D266-3), anti-CYP2E1 antibody (Millipore, Cat# 1252), and anti- β -actin (Cell Signaling Technology, Cat# 3700). To detect antigen-antibody complexes, peroxidase-conjugated anti-rabbit (Enzo Life Sciences, Cat# ADI-SAB-300-J) or anti-mouse (Enzo Life Sciences, Cat# ADI-SAB-100-J) or anti-rat (Santa Cruz Biotechnology Inc., Cat# sc-2032) secondary antibodies at a 1:3,000 dilution in a blocking buffer and incubated at room temperature for 1 h. Protein bands were visualized with enhanced chemiluminescence (ECL) detection system (Clarity™ Western ECL Substrate, Bio-Rad, CA, USA) using ImageQuant LAS 500 (GE Healthcare Life Science). Expression levels of protein were quantified using the ImageQuant TL software version 8.1.

Statistical analysis

All quantitative data obtained in experiments are subjected to statistical analyses and expressed as a mean \pm standard deviation (SD). Statistical analysis was performed using 2-sided unpaired Student's *t*-test between two groups or using one-way ANOVA with Tukey's post hoc test between three or more groups, as performed by GraphPad Prism 7.0 software (Graph Pad Software, San Diego, CA). Statistical significance was set at a value of $p < 0.05$. The sample size was predetermined based on the level of variation observed in the previous experiment. The experiments were done in an exploratory manner without testing a

prespecified statistical null hypothesis, and the *p*-value is explained for descriptive purposes.

Results

APAP treatment induces Mincle, SAP130, and pSyk expression in mouse liver

Intraperitoneal injection with APAP can induce liver damage dose-dependently. It was shown that hepatocellular necrosis and serum transaminase levels increased with an increase in the dose of APAP injection (Fig. 1A and B). To explore the effects of Mincle signaling on APAP hepatotoxicity, the expressions of Mincle, SAP130 (a ligand of Mincle), and related-downstream Mincle signaling molecules (pSyk and Syk) were measured. The mRNA expression of Mincle was markedly increased in the liver when mice were treated with either 300 or 500 mg/kg APAP (Fig. 1C). Additionally, protein levels of SAP130 and pSyk were substantially elevated, and mice treated with a dose of APAP at 300 mg/kg showed the highest hepatic protein levels of SAP130 and Syk phosphorylation (Fig. 1D). The Ct value of GAPDH and band intensity of β -actin were represented (Supplemental Fig. 1). These results showed that Mincle signaling was related to APAP-induced liver injury. Of note, since 500 mg/kg APAP is a lethal dose for mice and two of six mice in this group died in this experiment, a dose of APAP at 300 mg/kg was used in later experiments.

Mincle deletion ameliorates APAP-induced liver injury

In the present study, Mincle KO mice were used to determine the role of Mincle signaling in APAP hepatotoxicity, and Western blot analysis and genotype analysis were used to determine the generation of Mincle KO mice (Supplemental Fig. 2 and Supplemental Table 1). After injecting APAP into WT and Mincle KO mice, the results showed that hepatic necrosis in Mincle KO mice was markedly decreased when compared with WT mice (Fig. 2A). Similarly, decreased TUNEL positive nuclear bodies (Fig. 2B) and lower levels of serum aminotransferases (Fig. 2C) were found in APAP treated Mincle KO mice. These data

indicated that Mincle deletion ameliorated APAP hepatotoxicity.

Mincle increases the release of pro-inflammatory mediators without altering APAP metabolism in the injured liver

Liver injury induced by APAP is correlated with increased hepatic levels of pro-inflammatory cytokines. To examine whether mitigated toxicity in Mincle KO mice is associated with levels of pro-inflammatory mediators, hepatic levels of TNF- α , IL-1 β , IL-6 and MCP-1 were measured by ELISA. Compared with WT mice, hepatic levels of the cytokines were decreased in Mincle KO mice (Fig. 3A). CYP2E1 is essential for APAP metabolism with a potential to convert APAP into bio-activated NAPQI, which causes depletion of antioxidants such as GSH. The hepatic level of GSH and expression of CYP2E1 were examined in WT and Mincle KO mice to investigate whether the Mincle signaling was related to APAP metabolism. However, no statistically significant difference between the two types of mice in the hepatic level of GSH and the mRNA level of CYP2E1 was observed with APAP treatment (Fig. 3B and C). Moreover, no statistically significant difference between WT and Mincle KO mice was shown in the hepatic protein levels of CYP2E1 upon APAP treatment (Fig. 3D). The Ct value of GAPDH and band intensity of β -actin were represented (Supplemental Fig. 3). These results suggested that Mincle affected the expression of pro-inflammatory mediators but did not change APAP metabolism in the pathogenesis of APAP hepatotoxicity.

Mincle deficiency decreases the infiltration of neutrophils in the liver after APAP treatment

It is well known that the recruitment of neutrophils to the injured site is a characteristic event in APAP hepatotoxicity. Therefore, neutrophil infiltration was evaluated in this study.

The results showed that WT mice exhibited higher infiltration of intrahepatic neutrophils compared with Mincle KO mice after treatment with APAP (Fig. 4A). Consistently, immunohistochemical analyses revealed that the positive area of MPO, which is a neutrophil marker, was markedly decreased in APAP-treated Mincle KO mice (Fig. 4B). Furthermore, compared with WT mice, decreased expression of neutrophil attractant chemokines such as C-X-C motif chemokine ligand 1 (CXCL1) and CXCL2 were observed in the livers of Mincle KO mice (Fig. 4C). These data indicated that Mincle regulated intrahepatic neutrophil infiltration in APAP-treated mice.

Inhibition of Mincle downstream signaling attenuates APAP-induced liver injury

To further determine the role of the Mincle signaling pathway in APAP hepatotoxicity, WT mice were orally treated with GS9973, an inhibitor of Syk, before the administration of APAP. GS9973-treated mice showed lower hepatocellular necrosis (Fig. 5A) and decreased TUNEL positive areas (Fig. 5B), diminished serum levels of ALT and AST (Fig. 5C) compared with vehicle-treated mice. Consistently, inhibition of Syk signaling down-regulated hepatic levels of inflammatory cytokines, such as TNF- α and IL-1 β (Fig. 5D). Furthermore, GS9973 pretreated mice showed decreased infiltration of neutrophil and decreased positive area of MPO in the liver compared with mice without GS9973 treatment (Fig. 5E-H). Taken together, these findings revealed that the Mincle-Syk signaling pathway was crucial in the pathogenesis of hepatic injury induced by APAP.

Mincle signaling in KCs contributes to the liver injury induced by APAP

As parenchymal cells of liver, hepatocytes occupy most of the total liver volume and execute majority of the functions of the liver. In the present study, we found that primary hepatocytes from the WT and Mincle KO mice released a similar level of LDH with APAP

treatment (Supplemental Fig. 4). Subsequently, several cell populations from the liver of WT mice were isolated to determine the cellular source of Mincle. As shown in Fig. 6A, KCs expressed the highest level of Mincle, signifying that KCs were the major cellular sources of Mincle in the liver. Moreover, following the APAP challenge, the Mincle expression was dramatically up-regulated in KCs (Fig. 6B). Besides, GdCl₃-induced KCs-depleted Mincle KO mice showed similar histopathological lesions compared with KCs-depleted WT mice (Fig. 6C). The depletion of KCs was confirmed by flow cytometric analysis and qPCR (Supplemental Figure 5). Consistently, similar TUNEL positive areas and serum levels of aminotransferases were observed in KCs-depleted mice after treatment with APAP (Fig. 6D and E), indicating that KC depletion abolished the detrimental role of Mincle in APAP hepatotoxicity. The Ct value of GAPDH was represented (Supplemental Fig. 6).

To further investigate the effect of Mincle in KCs on the liver injury induced by APAP, we performed adoptive transfer experiments with F4/80⁺ KCs (Fig. 7A). The data showed that the adoptive transfer of KCs from WT donors partially reversed the hyporesponsiveness to APAP hepatotoxicity in Mincle KO mice, resulting in no statistically significant difference in histopathological lesions, aminotransferases levels, and the TUNEL positive area (Fig. 7B-D). Taken together, these results revealed that Mincle signaling was necessitated for the contribution of KCs in APAP-mediated liver injury.

Mincle signaling promotes the inflammatory response in KCs

Previous studies showed that activated KCs release a wide array of pro-inflammatory regulators during APAP hepatotoxicity to modulate liver injury (Krenkel et al., 2014; Jaeschke et al., 2012). We found that when compared with KCs from APAP-injected WT mice, those from APAP-injected Mincle KO mice had decreased mRNA expression levels of IL-1 β , CXCL1 and CXCL2 (Fig. 8A), which are involved in the inflammatory response and

neutrophil infiltration. Moreover, primary KCs treated with a Mincle ligand (TDB) had increased mRNA expressions of IL-1 β , CXCL1 and CXCL2 in WT groups compared with Mincle KO groups (Fig. 8B).

SAP130 released by injured hepatocytes is considered as the only non-pathogenic Mincle ligand with well-characterized characteristics (Greco et al., 2016). To further confirm whether Mincle ligand produced by injured hepatocytes affects the activation of KCs, we performed the experiments exploring the effects when KCs were exposed to conditioned media obtained from hepatocytes treated with APAP. As shown in Fig. 8C, the hepatocyte cultured media were prepared as control-conditioned media or APAP-conditioned media following 24 h incubation. The extremely increased cell damage was observed at 12 and 24 h in hepatocytes cultured with APAP (Supplemental Fig. 7), and the level of released SAP130 in APAP-conditioned media was increased when compared with those in control-conditioned media (Supplemental Fig. 8). The conditioned media were mixed with fresh media and used to stimulate primary KCs (Fig. 8C). Results showed that WT KCs cultured in APAP-conditioned media exhibited substantially higher expressions of IL-1 β , CXCL1 and CXCL2 when compared with Mincle KO KCs (Fig. 8D). The Ct value of GAPDH was represented (Supplemental Fig. 9). Collectively, these data suggested that stimulating Mincle signaling promoted the inflammatory response in KCs.

Discussion

The evidence from this study suggests that Mincle deletion and subsequent downstream molecular inhibition attenuates the liver injury induced by APAP. In particular, Mincle in KCs plays a vital role in the progression of APAP hepatotoxicity. Consequently, the findings provide a valuable therapeutic target in acute liver injury and provide insights into the relevance of Mincle in APAP hepatotoxicity.

APAP is one of the most frequent drugs to induce acute liver injury, and the injury phases can be divided into two steps (Bhushan and Apte, 2019). The first step is to initiate APAP hepatotoxicity, which involves CYP2E1 mediated catalysis of APAP to a highly toxic metabolite NAPQI, and the toxicity of NAPQI can be relieved by binding to GSH. The second step is sterile inflammation, which is triggered by DAMPs released by necrotic hepatocytes. It is well described that before APAP administration in a mouse model, a duration of fasting period between 12 and 16 h could deplete hepatocytic GSH and create comparable conditions for APAP metabolism (Mossanen and Tacke, 2015). Prolonged fasting period could enhance the susceptibility of mouse liver to APAP through decreasing hepatic GSH concentrations and detoxification capacity of the liver (Strubelt et al., 1981). Although Kataoka *et al.* have shown that Mincle-deficient mice developed a similar ALT level as WT mice after treatment with APAP, the differences in fasting duration compared to our study may contribute to the resultant discrepancy in results (Kataoka et al., 2014). In the latter study, the mice were prohibited from eating food for 18 h before and 4 h after APAP injection. The prolonged fasting time may lead to an aggravation of APAP hepatotoxicity, which could induce some compensatory change in Mincle KO mice (Kataoka et al., 2014) or triggered the inflammation by other signalings such as toll-like receptor signalings (Salama et al., 2015). These results raise a possible hypothesis that the role of Mincle is correlated with the degree of APAP initial hepatotoxicity, and this hypothesis needs to be verified by further research.

In this study, similar levels of GSH and CYP2E1 in the liver were observed in WT and Mincle KO mice, suggesting that Mincle does not substantially modulate the metabolism of APAP. This may explain by the high expression of Mincle in immune cells but conspicuous absence in hepatocytes (Greco et al., 2016). Of note, we found that KCs expressed the highest

level of Mincle in the liver, and APAP induced injured livers showed increased expression of Mincle in KCs. The main source of pro-inflammatory cytokines in the liver is believed to be KCs known as residential macrophages (Ju et al., 2002). Our results showed similar severity of APAP-hepatotoxicity between KC-depleting WT mice and KC-depleting Mincle KO mice, indicating that KCs are required for the detrimental role of Mincle in APAP hepatotoxicity. Connolly et al. (2011) have shown that DC protects against APAP-mediated liver injury; our findings showed that DCs had a high expression of Mincle. The Mincle expressed in DCs is demonstrated to be activated by stimuli from fungi, mycobacteria or even parasites, and is well related to T cell differentiation and activation (Negi et al., 2019; Martinez-Lopez et al., 2019; Iborra et al., 2016). A recent study has reported that Mincle-Syk axis in DCs could sense mucosal-associated bacteria and induce the release of cytokines such as IL-6, resulting in enhanced intestinal immune barrier function (Martinez-Lopez et al., 2019). Therefore, we believe that Mincle may exert a distinct role depending on specific cell types and different disease models.

In the present study, Mincle was demonstrated as an important modulator of KC activation. This notion was advocated by a previous study showing that SAP130 was able to extremely increase the production of pro-inflammatory mediators in WT macrophages primed by low-dose LPS (Zhou et al., 2016). Although the accurate role of KCs in the progression of acute liver injury remains controversial according to the literature (Ju et al., 2002), it is well accepted that KCs activated by DAMPs could trigger and inappropriately amplify inflammation (Yang and Tennessean, 2019). A great deal of evidence has shown that the activation of the nucleotide-binding domain and leucine-rich repeat protein 3 (NLRP3) inflammasome is required for the Mincle-induced Syk-mediated up-regulation of cytokine production (Schweneker et al., 2013; Gross et al., 2009; Zhang et al., 2015). A previous study

also showed that NLRP3-deficient KCs treated with SAP130 had decreased expression of IL-1 β compared with WT KCs (Kim et al., 2018). Furthermore, de Castro-Jorge et al. (2019) have reported that the levels of cytokines and the population of infiltrated neutrophils were decreased in the footpad of Mayaro virus-infected NLRP3 deficient-mice. Therefore, further study is needed to explore whether an NLRP3-dependent manner is involved in the detrimental role of Mincle in APAP hepatotoxicity.

Collectively, as shown in the schematic (Fig. 9), the present work indicates a regulatory role of Mincle in KC activation, which contributes to the full progression of liver injury induced by APAP. It is hypothesized that understanding this mechanism will offer valuable insights to overcome the limitation of APAP hepatotoxicity treatment.

Authorship Contributions

Participated in research design: Zhao, J. W. Kim, Han, B. Kim.

Conducted experiments: Zhao, J. W. Kim, Zhou, Tian.

Performed data analysis: Zhao, Qi, Lim.

Wrote or contributed to the writing of the manuscript: Zhao, Zhou, B. Kim.

References

- Bhushan B and Apte U (2019) Liver Regeneration after Acetaminophen Hepatotoxicity: Mechanisms and Therapeutic Opportunities. *Am J Pathol* **189**(4): 719-729.
- Brown GD (2008) Sensing necrosis with Mincle. *Nat Immunol* **9**(10): 1099-1100.
- Chatterjee S, Ganini D, Tokar EJ, Kumar A, Das S, Corbett J, Kadiiska MB, Waalkes MP, Diehl AM and Mason RP (2013) Leptin is key to peroxynitrite-mediated oxidative stress and Kupffer cell activation in experimental non-alcoholic steatohepatitis. *J Hepatol* **58**(4): 778-784.
- Chen L, Wang P, Manautou JE and Zhong XB (2020) Knockdown of Long Noncoding RNAs Hepatocyte Nuclear Factor 1alpha Antisense RNA 1 and Hepatocyte Nuclear Factor 4alpha Antisense RNA 1 Alters Susceptibility of Acetaminophen-Induced Cytotoxicity in HepaRG Cells. *Mol Pharmacol* **97**(4): 278-286.
- Chun LJ, Tong MJ, Busuttill RW and Hiatt JR (2009) Acetaminophen hepatotoxicity and acute liver failure. *J Clin Gastroenterol* **43**(4): 342-349.
- Connolly MK, Ayo D, Malhotra A, Hackman M, Bedrosian AS, Ibrahim J, Cieza-Rubio NE, Nguyen AH, Henning JR, Dorvil-Castro M, Pachter HL and Miller G (2011) Dendritic cell depletion exacerbates acetaminophen hepatotoxicity. *Hepatology* **54**(3): 959-968.
- Currie KS, Kropf JE, Lee T, Blomgren P, Xu J, Zhao Z, Gallion S, Whitney JA, Maclin D, Lansdon EB, Maciejewski P, Rossi AM, Rong H, Macaluso J, Barbosa J, Di Paolo JA and Mitchell SA (2014) Discovery of GS-9973, a selective and orally efficacious inhibitor of spleen tyrosine kinase. *J Med Chem* **57**(9): 3856-3873.
- de Castro-Jorge LA, de Carvalho RVH, Klein TM, Hiroki CH, Lopes AH, Guimaraes RM, Fumagalli MJ, Floriano VG, Agostinho MR, Slhessarenko RD, Ramalho FS, Cunha TM, Cunha FQ, da Fonseca BAL and Zamboni DS (2019) The NLRP3 inflammasome is involved with the pathogenesis of Mayaro virus. *PLoS Pathog* **15**(9): e1007934.
- de Rivero Vaccari JC, Brand FJ, 3rd, Berti AF, Alonso OF, Bullock MR and de Rivero Vaccari JP (2015) Mincle signaling in the innate immune response after traumatic brain injury. *J Neurotrauma* **32**(4): 228-236.
- Greco SH, Torres-Hernandez A, Kalabin A, Whiteman C, Rokosh R, Ravirala S, Ochi A, Gutierrez J, Salyana MA, Mani VR, Nagaraj SV, Deutsch M, Seifert L, Daley D, Barilla R, Hundeyin M, Nikifrov Y, Tejada K, Gelb BE, Katz SC and Miller G (2016) Mincle Signaling Promotes Con A Hepatitis. *J Immunol* **197**(7): 2816-2827.
- Gross O, Poock H, Bscheider M, Dostert C, Hanneschlager N, Endres S, Hartmann G, Tardivel A, Schweighoffer E, Tybulewicz V, Mocsai A, Tschopp J and Ruland J (2009) Syk kinase signalling couples to the Nlrp3 inflammasome for anti-fungal host defence. *Nature* **459**(7245): 433-436.
- He Y, Xu L, Li B, Guo ZN, Hu Q, Guo Z, Tang J, Chen Y, Zhang Y, Tang J and Zhang JH (2015) Macrophage-Inducible C-Type Lectin/Spleen Tyrosine Kinase Signaling Pathway Contributes to Neuroinflammation After Subarachnoid Hemorrhage in Rats. *Stroke* **46**(8):

2277-2286.

- Holt MP, Cheng L and Ju C (2008) Identification and characterization of infiltrating macrophages in acetaminophen-induced liver injury. *J Leukoc Biol* **84**(6): 1410-1421.
- Iborra S, Martinez-Lopez M, Cueto FJ, Conde-Garrosa R, Del Fresno C, Izquierdo HM, Abram CL, Mori D, Campos-Martin Y, Reguera RM, Kemp B, Yamasaki S, Robinson MJ, Soto M, Lowell CA and Sancho D (2016) Leishmania Uses Mincle to Target an Inhibitory ITAM Signaling Pathway in Dendritic Cells that Dampens Adaptive Immunity to Infection. *Immunity* **45**(4): 788-801.
- Ishikawa E, Ishikawa T, Morita YS, Toyonaga K, Yamada H, Takeuchi O, Kinoshita T, Akira S, Yoshikai Y and Yamasaki S (2009) Direct recognition of the mycobacterial glycolipid, trehalose dimycolate, by C-type lectin Mincle. *J Exp Med* **206**(13): 2879-2888.
- Jaeschke H and Bajt ML (2006) Intracellular signaling mechanisms of acetaminophen-induced liver cell death. *Toxicol Sci* **89**(1): 31-41.
- Jaeschke H, Ramachandran A, Chao X and Ding WX (2019) Emerging and established modes of cell death during acetaminophen-induced liver injury. *Arch Toxicol* **93**(12): 3491-3502.
- Jaeschke H, Williams CD, Ramachandran A and Bajt ML (2012) Acetaminophen hepatotoxicity and repair: the role of sterile inflammation and innate immunity. *Liver Int* **32**(1): 8-20.
- Ju C, Reilly TP, Bourdi M, Radonovich MF, Brady JN, George JW and Pohl LR (2002) Protective role of Kupffer cells in acetaminophen-induced hepatic injury in mice. *Chem Res Toxicol* **15**(12): 1504-1513.
- Kataoka H, Kono H, Patel Z, Kimura Y and Rock KL (2014) Evaluation of the contribution of multiple DAMPs and DAMP receptors in cell death-induced sterile inflammatory responses. *PLoS One* **9**(8): e104741.
- Kim JW, Roh YS, Jeong H, Yi HK, Lee MH, Lim CW and Kim B (2018) Spliceosome-Associated Protein 130 Exacerbates Alcohol-Induced Liver Injury by Inducing NLRP3 Inflammasome-Mediated IL-1beta in Mice. *Am J Pathol* **188**(4): 967-980.
- Krenkel O, Mossanen JC and Tacke F (2014) Immune mechanisms in acetaminophen-induced acute liver failure. *Hepatobiliary Surg Nutr* **3**(6): 331-343.
- Lancaster EM, Hiatt JR and Zarrinpar A (2015) Acetaminophen hepatotoxicity: an updated review. *Arch Toxicol* **89**(2): 193-199.
- Larsen FS and Wendon J (2014) Understanding paracetamol-induced liver failure. *Intensive Care Med* **40**(6): 888-890.
- Larson AM, Polson J, Fontana RJ, Davern TJ, Lalani E, Hynan LS, Reisch JS, Schiodt FV, Ostapowicz G, Shakil AO, Lee WM and Acute Liver Failure Study G (2005) Acetaminophen-induced acute liver failure: results of a United States multicenter, prospective study. *Hepatology* **42**(6): 1364-1372.
- Lawson JA, Farhood A, Hopper RD, Bajt ML and Jaeschke H (2000) The hepatic inflammatory response after acetaminophen overdose: role of neutrophils. *Toxicol Sci* **54**(2): 509-516.
- Lee WB, Kang JS, Yan JJ, Lee MS, Jeon BY, Cho SN and Kim YJ (2012) Neutrophils Promote

- Mycobacterial Trehalose Dimycolate-Induced Lung Inflammation via the Mincle Pathway. *PLoS Pathog* **8**(4): e1002614.
- Lin J, He K, Zhao G, Li C, Hu L, Zhu G, Niu Y and Hao G (2017) Mincle inhibits neutrophils and macrophages apoptosis in *A. fumigatus* keratitis. *Int Immunopharmacol* **52**: 101-109.
- Martin-Murphy BV, Holt MP and Ju C (2010) The role of damage associated molecular pattern molecules in acetaminophen-induced liver injury in mice. *Toxicol Lett* **192**(3): 387-394.
- Martinez-Lopez M, Iborra S, Conde-Garrosa R, Mastrangelo A, Danne C, Mann ER, Reid DM, Gaboriau-Routhiau V, Chaparro M, Lorenzo MP, Minnerup L, Saz-Leal P, Slack E, Kemp B, Gisbert JP, Dzionek A, Robinson MJ, Ruperez FJ, Cerf-Bensussan N, Brown GD, Bernardo D, LeibundGut-Landmann S and Sancho D (2019) Microbiota Sensing by Mincle-Syk Axis in Dendritic Cells Regulates Interleukin-17 and -22 Production and Promotes Intestinal Barrier Integrity. *Immunity* **50**(2): 446-461 e449.
- Matsumoto M, Tanaka T, Kaisho T, Sanjo H, Copeland NG, Gilbert DJ, Jenkins NA and Akira S (1999) A novel LPS-inducible C-type lectin is a transcriptional target of NF-IL6 in macrophages. *J Immunol* **163**(9): 5039-5048.
- Merlin S, Bhargava KK, Ranaldo G, Zanolini D, Palestro CJ, Santambrogio L, Prat M, Follenzi A and Gupta S (2016) Kupffer Cell Transplantation in Mice for Elucidating Monocyte/Macrophage Biology and for Potential in Cell or Gene Therapy. *Am J Pathol* **186**(3): 539-551.
- Michel MC, Murphy TJ and Motulsky HJ (2020) New Author Guidelines for Displaying Data and Reporting Data Analysis and Statistical Methods in Experimental Biology. *Mol Pharmacol* **97**(1): 49-60.
- Mossanen JC and Tacke F (2015) Acetaminophen-induced acute liver injury in mice. *Lab Anim* **49**(1 Suppl): 30-36.
- Negi S, Pahari S, Bashir H and Agrewala JN (2019) Gut Microbiota Regulates Mincle Mediated Activation of Lung Dendritic Cells to Protect Against Mycobacterium tuberculosis. *Front Immunol* **10**: 1142.
- Prescott LF, Park J, Ballantyne A, Adriaenssens P and Proudfoot AT (1977) Treatment of paracetamol (acetaminophen) poisoning with N-acetylcysteine. *Lancet* **2**(8035): 432-434.
- Richardson MB and Williams SJ (2014) MCL and Mincle: C-Type Lectin Receptors That Sense Damaged Self and Pathogen-Associated Molecular Patterns. *Front Immunol* **5**: 288.
- Salama M, Elgamal M, Abdelaziz A, Ellithy M, Magdy D, Ali L, Fekry E, Mohsen Z, Mostafa M, Elgamal H, Sheashaa H and Sobh M (2015) Toll-like receptor 4 blocker as potential therapy for acetaminophen-induced organ failure in mice. *Exp Ther Med* **10**(1): 241-246.
- Schwenker K, Gorka O, Schwenker M, Poeck H, Tschopp J, Peschel C, Ruland J and Gross O (2013) The mycobacterial cord factor adjuvant analogue trehalose-6,6'-dibehenate (TDB) activates the Nlrp3 inflammasome. *Immunobiology* **218**(4): 664-673.
- Smilkstein MJ, Knapp GL, Kulig KW and Rumack BH (1988) Efficacy of oral N-acetylcysteine in the treatment of acetaminophen overdose. Analysis of the national multicenter study (1976 to 1985). *N Engl J Med* **319**(24): 1557-1562.

- Strubelt O, Dost-Kempf E, Siegers CP, Younes M, Volpel M, Preuss U and Dreckmann JG (1981) The influence of fasting on the susceptibility of mice to hepatotoxic injury. *Toxicol Appl Pharmacol* **60**(1): 66-77.
- Wu J, Li J, Salcedo R, Mivechi NF, Trinchieri G and Horuzsko A (2012) The proinflammatory myeloid cell receptor TREM-1 controls Kupffer cell activation and development of hepatocellular carcinoma. *Cancer Res* **72**(16): 3977-3986.
- Yamasaki S, Ishikawa E, Sakuma M, Hara H, Ogata K and Saito T (2008) Mincle is an ITAM-coupled activating receptor that senses damaged cells. *Nat Immunol* **9**(10): 1179-1188.
- Yang R and Tonnesseen TI (2019) DAMPs and sterile inflammation in drug hepatotoxicity. *Hepatol Int* **13**(1): 42-50.
- Zaher H, Buters JT, Ward JM, Bruno MK, Lucas AM, Stern ST, Cohen SD and Gonzalez FJ (1998) Protection against acetaminophen toxicity in CYP1A2 and CYP2E1 double-null mice. *Toxicol Appl Pharmacol* **152**(1): 193-199.
- Zhang Z, He L, Hu S, Wang Y, Lai Q, Yang P, Yu Q, Zhang S, Xiong F, Simseyilmaz S, Ning Q, Li J, Zhang D, Zhang H, Xiang X, Zhou Z, Sun H and Wang CY (2015) AAL exacerbates pro-inflammatory response in macrophages by regulating Mincle/Syk/Card9 signaling along with the Nlrp3 inflammasome assembly. *Am J Transl Res* **7**(10): 1812-1825.
- Zhao J, Park S, Kim JW, Qi J, Zhou Z, Lim CW and Kim B (2020) Nicotine attenuates concanavalin A-induced liver injury in mice by regulating the alpha7-nicotinic acetylcholine receptor in Kupffer cells. *Int Immunopharmacol* **78**: 106071.
- Zhou H, Yu M, Zhao J, Martin BN, Roychowdhury S, McMullen MR, Wang E, Fox PL, Yamasaki S, Nagy LE and Li X (2016) IRAKM-Mincle axis links cell death to inflammation: Pathophysiological implications for chronic alcoholic liver disease. *Hepatology* **64**(6): 1978-1993.

Footnotes

This research was supported by Basic Science Research Program through the National Research Foundation (NRF) funded by the Ministry of Education (2017R1D1A3B03030521) and by the Korean government (MSIT) (2020R1A2C1007178). Jing Zhao also gratefully acknowledges the financial support from the China Scholarship Council (CSC, File No. 201608260078).

Figure legends

Fig. 1 The expression of Mincle signaling genes in acetaminophen (APAP)-induced liver injury. Wild-type (WT) male mice were injected with pyrogen-free phosphate-buffered saline (PBS) ($n = 5$) or APAP (150, 300, or 500 mg/kg) ($n = 6$) and samples were harvested at 24 h. **A** Representative histological liver sections stained with H&E are shown. **B** Serum levels of ALT and AST were measured. **C** Hepatic mRNA expression levels of Mincle were measured by quantitative real-time PCR and data are shown as fold change compared with the relative expression of Mincle in PBS injected mice. **D** Western blot analysis was performed using pSyk, Syk and SAP130 antibodies. Data are presented as mean \pm SD. A one-way ANOVA with Tukey's post hoc test was performed in **B**, **C** and **D**. * $p < 0.05$, ** $p < 0.01$, *** $p < 0.001$ vs. the indicated groups.

Fig. 2 The effect of Mincle deficiency in acetaminophen (APAP)-induced liver injury. Mice were administered with PBS (Cont) ($n = 5$) or APAP (300 mg/kg) ($n = 8$) and samples were harvested at 24 h. **A** Representative histological liver sections stained with H&E are shown. **B** Apoptosis was determined by TUNEL staining and quantification of TUNEL-positive area. **C** Serum levels of ALT and AST were measured for each cohort. Data are presented as mean \pm SD. A t -test was performed in **B** and **C**. ** $p < 0.01$, *** $p < 0.001$ vs. the indicated groups. MKO, Mincle KO.

Fig. 3 Role of Mincle in acetaminophen (APAP)-induced inflammatory responses and oxidative stress in liver. Mice were administered with PBS (Cont) or APAP (300 mg/kg) and liver samples were collected at 24 h. **A** Intrahepatic cytokine levels of TNF- α , IL-1 β , IL-6, and MCP-1 were measured by ELISA. **B** Intrahepatic level of GSH was measured by ELISA. **C** Intrahepatic mRNA expression of CYP2E1 was measured by quantitative real-time PCR

and shown as fold change in comparison with the PBS injected WT mice. **D** Intrahepatic protein level of CYP2E1 was determined by Western blot analysis. Data are presented as mean \pm SD. A *t*-test was performed in **A-D**. ** $p < 0.01$ vs. the indicated groups, *NS*, no significant difference. MKO, Mincle KO.

Fig. 4 Role of Mincle in acetaminophen (APAP)-induced neutrophils infiltration in liver. Mice were administered with PBS (Cont) or APAP (300 mg/kg) and liver samples were collected at 24 h. **A-B** Flow cytometric analysis ($n = 4$ in Cont group and $n = 5$ in APAP group) and immunohistochemical staining ($n = 5$ in Cont group and $n = 8$ in APAP group) were performed to evaluate neutrophil accumulation in livers of WT and Mincle KO mice. **C** Hepatic mRNA levels of CXCL1 and CXCL2 were measured by quantitative real-time PCR and shown as fold change in comparison with the PBS injected WT mice ($n = 5$ in Cont group and $n = 8$ in APAP group). Data are presented as mean \pm SD. A *t*-test was performed in **A-C**. * $p < 0.05$, ** $p < 0.01$, *** $p < 0.001$ vs. the indicated groups. MKO, Mincle KO; MPO, myeloperoxidase.

Fig. 5 The effect of Mincle downstream signaling blockade in acetaminophen (APAP)-induced liver injury. WT mice were injected with PBS (Cont) ($n = 6$) or APAP (300 mg/kg) ($n = 6$) with or without the Syk inhibitor GS9973. Samples were collected at 24 h after APAP injection. **A** Representative histological liver sections stained with H&E are shown. **B** Apoptosis was determined by TUNEL staining and quantification of TUNEL-positive area. **C** Serum levels of ALT and AST were measured for each cohort. **D** Intrahepatic cytokine levels of TNF- α and IL-1 β were measured by ELISA. **E-H** Flow cytometric analysis and immunohistochemical staining were performed to evaluate neutrophil accumulation in mice livers. Data are presented as mean \pm SD. A *t*-test was performed in **B-D**, **G-H**. * $p < 0.05$, ** $p < 0.01$, *** $p < 0.001$ vs. the indicated groups. MPO, myeloperoxidase.

Fig. 6 Role of Kupffer cells (KCs) in the detrimental effect of Mincle in acetaminophen (APAP)-induced liver injury. **A** Relative mRNA levels of Mincle were measured in isolated liver cell fractions, including hepatocytes, neutrophils, Kupffer cells (KCs), and dendritic cells (DCs) in WT mice. Data are shown as fold change compared with the relative expression of Mincle in hepatocytes. **B** Mice were treated with PBS (Cont) or APAP (300 mg/kg). KCs were isolated at the indicated times and relative mRNA levels of Mincle were measured. Data are shown as fold change compared with the relative expression of Mincle in control KCs. **C-E** Mice were intravenously injected with saline as vehicle ($n = 5$) or GdCl_3 ($n = 5$) to deplete KCs. Subsequently, APAP (300 mg/kg) was injected into mice for 24 h. **C** Representative histological liver sections stained with H&E are shown. **D** Apoptosis was determined by TUNEL staining and quantification of TUNEL-positive area. **E** Serum levels of ALT and AST were measured. Data are presented as mean \pm SD. A one-way ANOVA with Tukey's post hoc test was performed in **A-B** and t -test was performed in **D** and **E**. * $p < 0.05$, ** $p < 0.01$, *** $p < 0.001$ vs. the indicated groups. MKO, Mincle KO.

Fig. 7 Role of Mincle signaling in Kupffer cells (KCs) in acetaminophen (APAP)-induced liver injury. **A** WT mice ($n = 4$) and Mincle KO mice ($n = 4$) were depleted of KCs and adoptively transferred with F4/80^+ KCs (1×10^6 cells, i.v.) harvested from WT mice. Mice were then injected with APAP (300 mg/kg) and sacrificed at 24 h. **B** Representative histological liver sections stained with H&E are shown. **C** Serum levels of ALT and AST were measured. **D** Apoptosis was determined by TUNEL staining and quantification of TUNEL-positive area. Data are presented as mean \pm SD. A t -test was performed in **C** and **D**. *NS*, no significant difference.

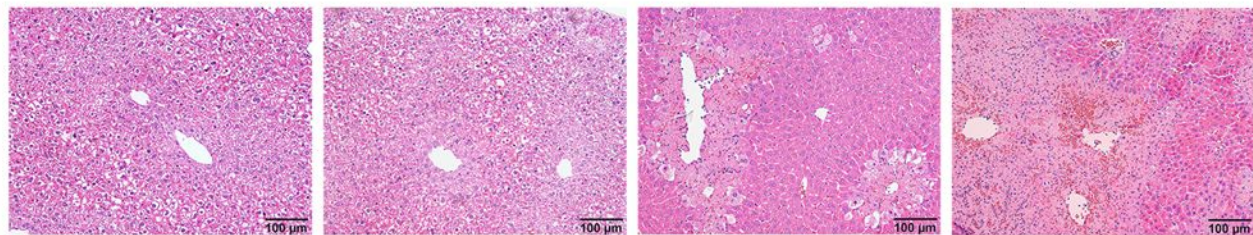
Fig. 8 Role of Mincle signaling in the activation of Kupffer cells (KCs). **A** KCs were isolated from livers of the two types of mice after PBS (Cont) or APAP (300 mg/kg) injection for 24 h.

Relative mRNA levels of IL-1 β , CXCL1 and CXCL2 were measured by real-time quantitative PCR and shown as fold change in comparison with the PBS injected WT mice. **B** Primary KCs isolated from WT and Mincle KO (MKO) mice were treated with Mincle ligand (TDB, 4 μ g/mL) for 24 h. Relative mRNA levels of IL-1 β , CXCL1 and CXCL2 were measured by quantitative real-time PCR and shown as fold change in comparison with control WT-KCs. **C** Hepatocytes were isolated from WT mice and cultured in media with or without APAP (10 mM). The supernatant was collected as conditioned media at 24 h. Diluted conditioned media with fresh media was used to stimulate the KCs from WT or Mincle KO mice for 2 h. **D** Relative mRNA levels of IL-1 β , CXCL1 and CXCL2 in KCs were measured by quantitative real-time PCR and shown as fold change in comparison with WT KCs treated with control conditioned media. Data are presented as mean \pm SD ($n = 3$ independent experiments). A t -test was performed in **A**, **B** and **D**. * $p < 0.05$, ** $p < 0.01$, *** $p < 0.001$ vs. the indicated groups, *NS*, no significant difference.

Fig. 9 Schematic presentation showing the detrimental role of Mincle in APAP-induced liver injury. Mincle signaling activates Kupffer cells to produce pro-inflammatory mediators, which in turn promote hepatocyte damage and neutrophil infiltration. Thus, manipulating the Mincle signaling might be useful as a novel therapeutic strategy to treat APAP-induced liver injury.

Table 1. Sequences of mouse primers used in qPCR

Gene	Primer sequences-Forward	Primer sequences-Reverse
Mincle	5'-AACCCACTCTATCTGCTCAGTGCTT-3'	5'-CCAGCATGAATGGCATGGA-3'
IL-1β	5'-CTCGCAGCAGCACATCAACA-3'	5'-CCACGGGAAAGACACAGGTA-3'
CYP2E1	5'-AAGCGCTTCGGGCCAG-3'	5'-TAGCCATGCAGGACCACGA-3'
CXCL1	5'-TGCACCCAAACCGAAGTC-3'	5'-GTCAGAAGCCAGCGTTCACC-3'
CXCL2	5'-GCCAAGGGTTGACTTCAAGAACA-3'	5'-AGGCTCCTCCTTCCAGGTCA-3'
GAPDH	5'-ACGGCAAATTCAACGGCACAG-3'	5'-AGACTCCACGACATACTCAGCAC-3'

A

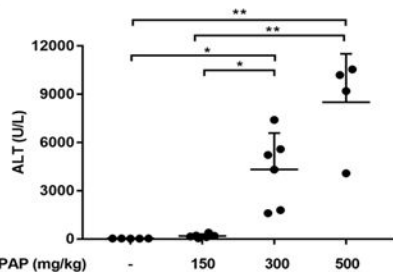
APAP (mg/kg)

-

150

300

500

B

ALT (U/L)

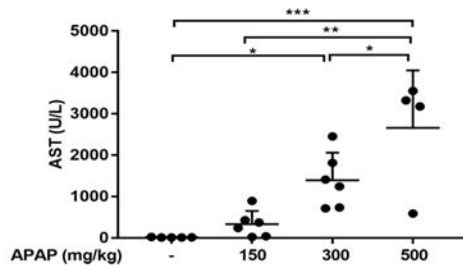
APAP (mg/kg)

-

150

300

500



AST (U/L)

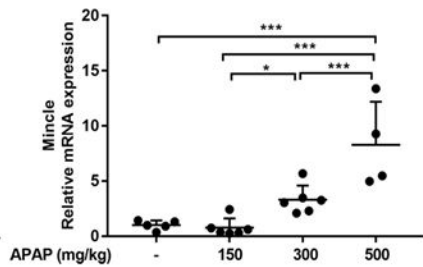
APAP (mg/kg)

-

150

300

500

CMincle
Relative mRNA expression

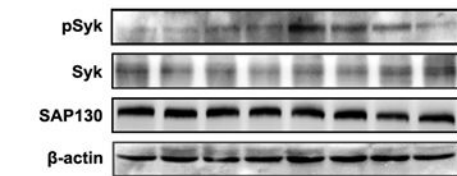
APAP (mg/kg)

-

150

300

500

D

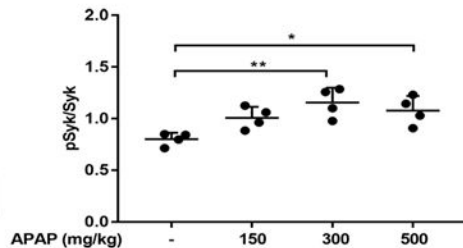
APAP (mg/kg)

-

150

300

500



pSyk/Syk

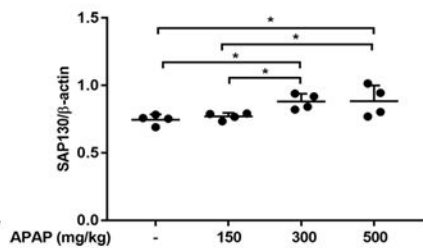
APAP (mg/kg)

-

150

300

500



SAP130/β-actin

APAP (mg/kg)

-

150

300

500

Figure 1

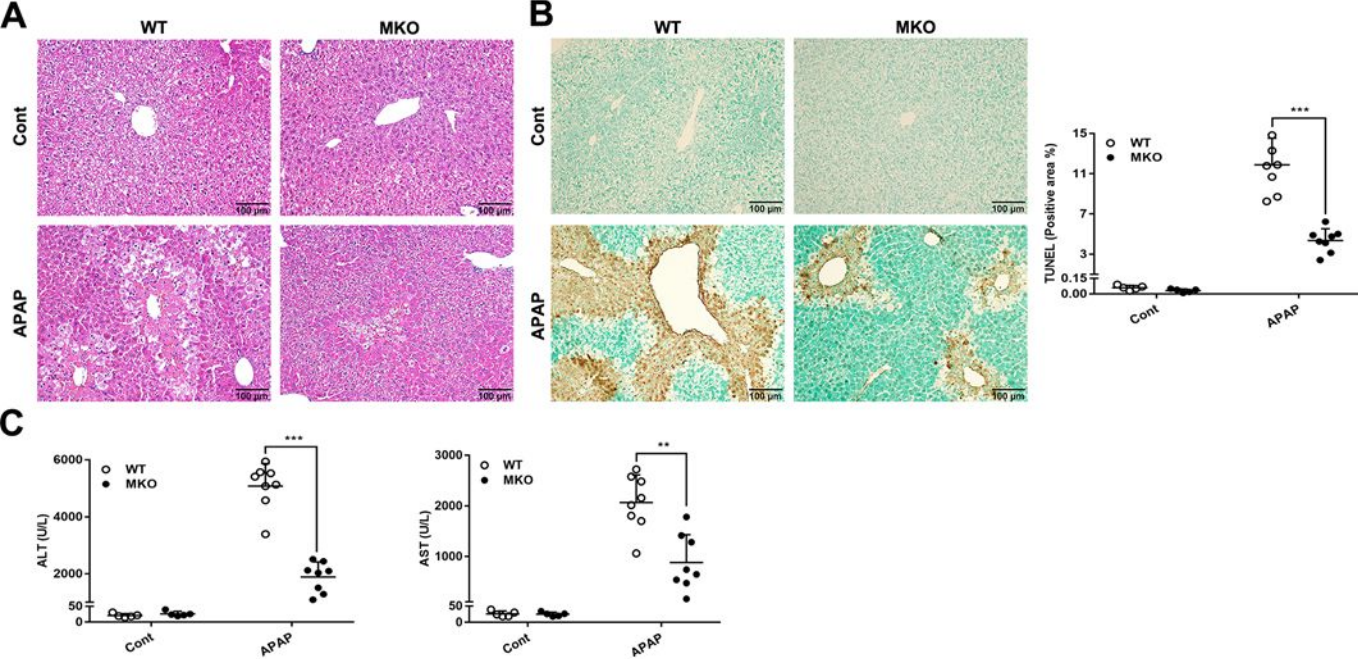


Figure 2

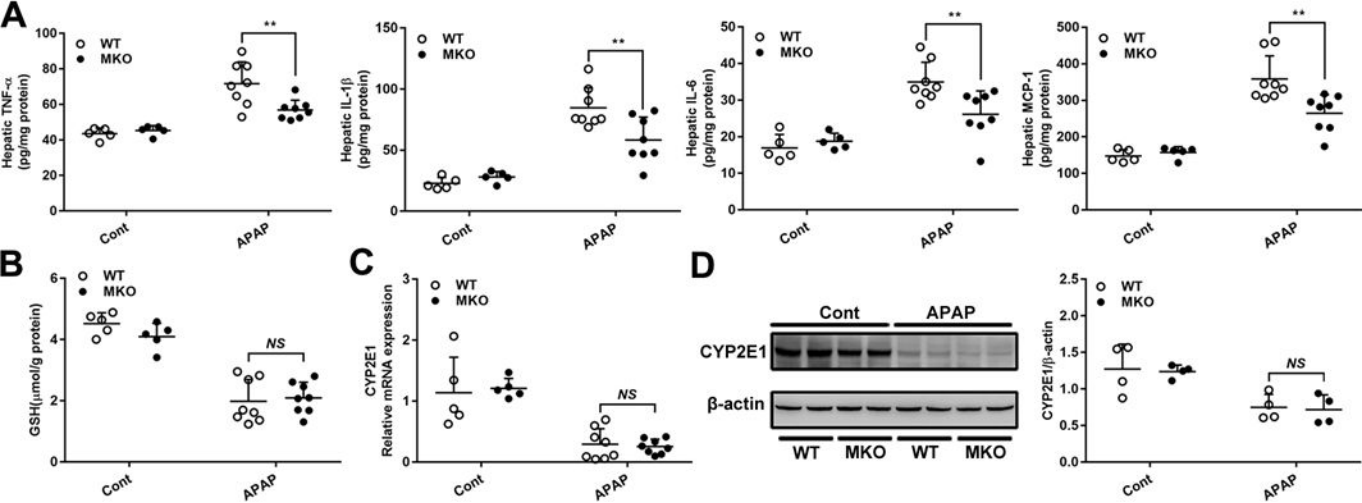


Figure 3

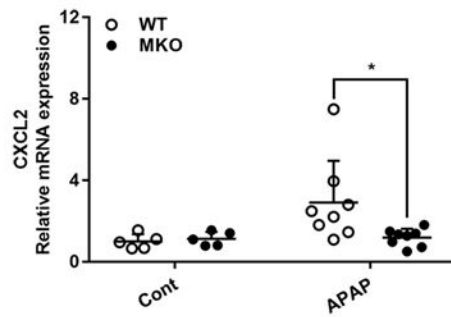
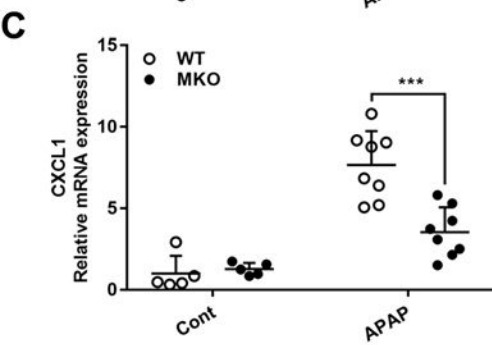
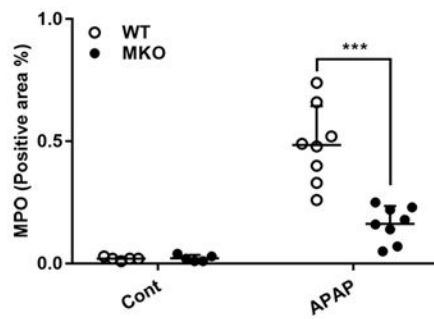
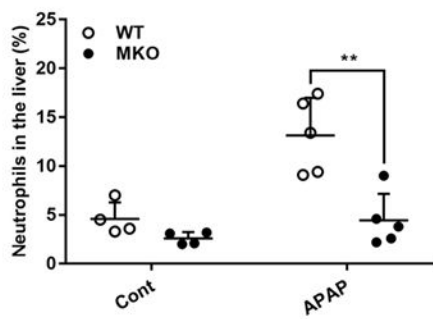
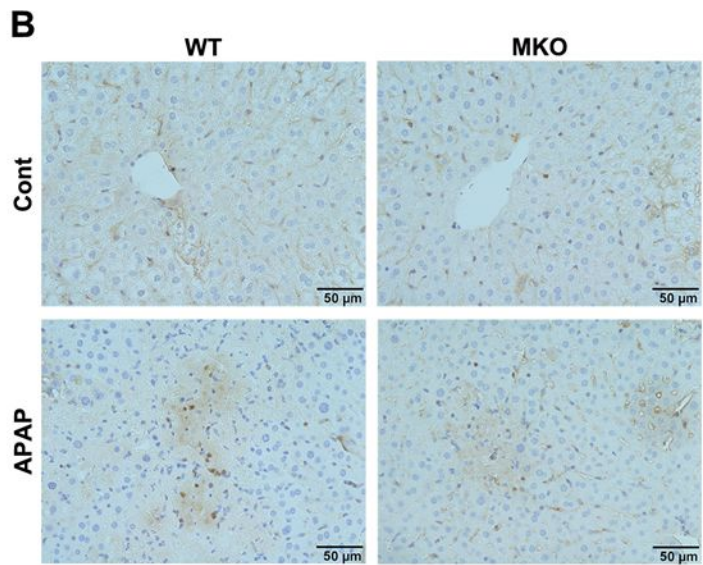
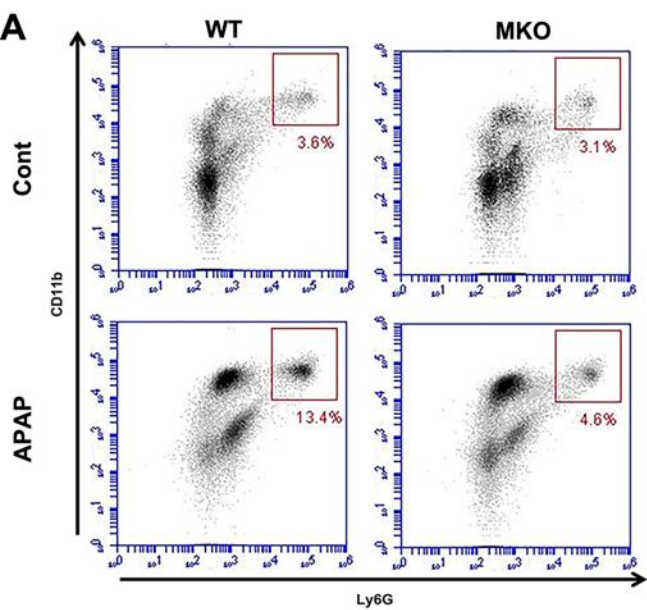


Figure 4

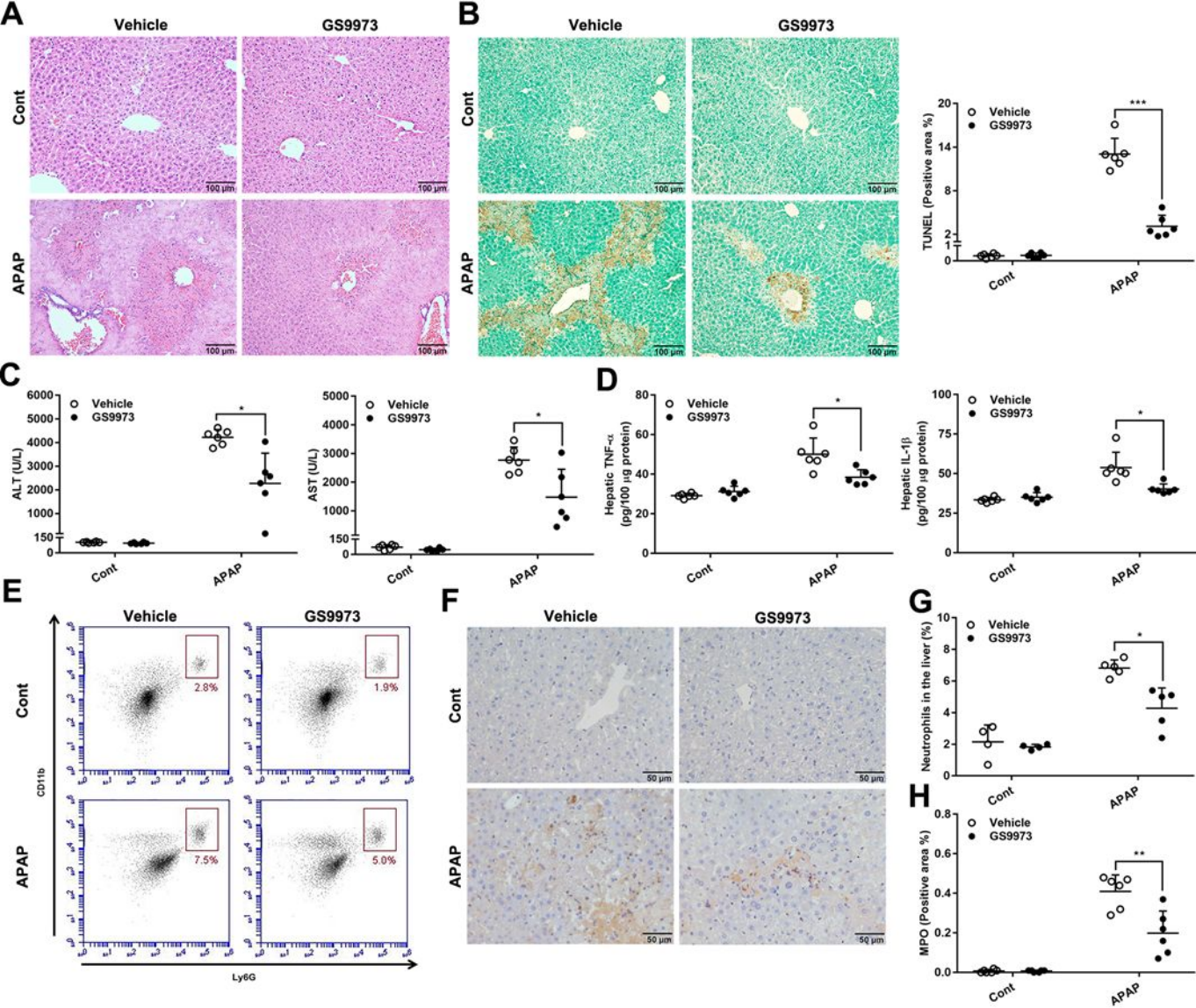


Figure 5

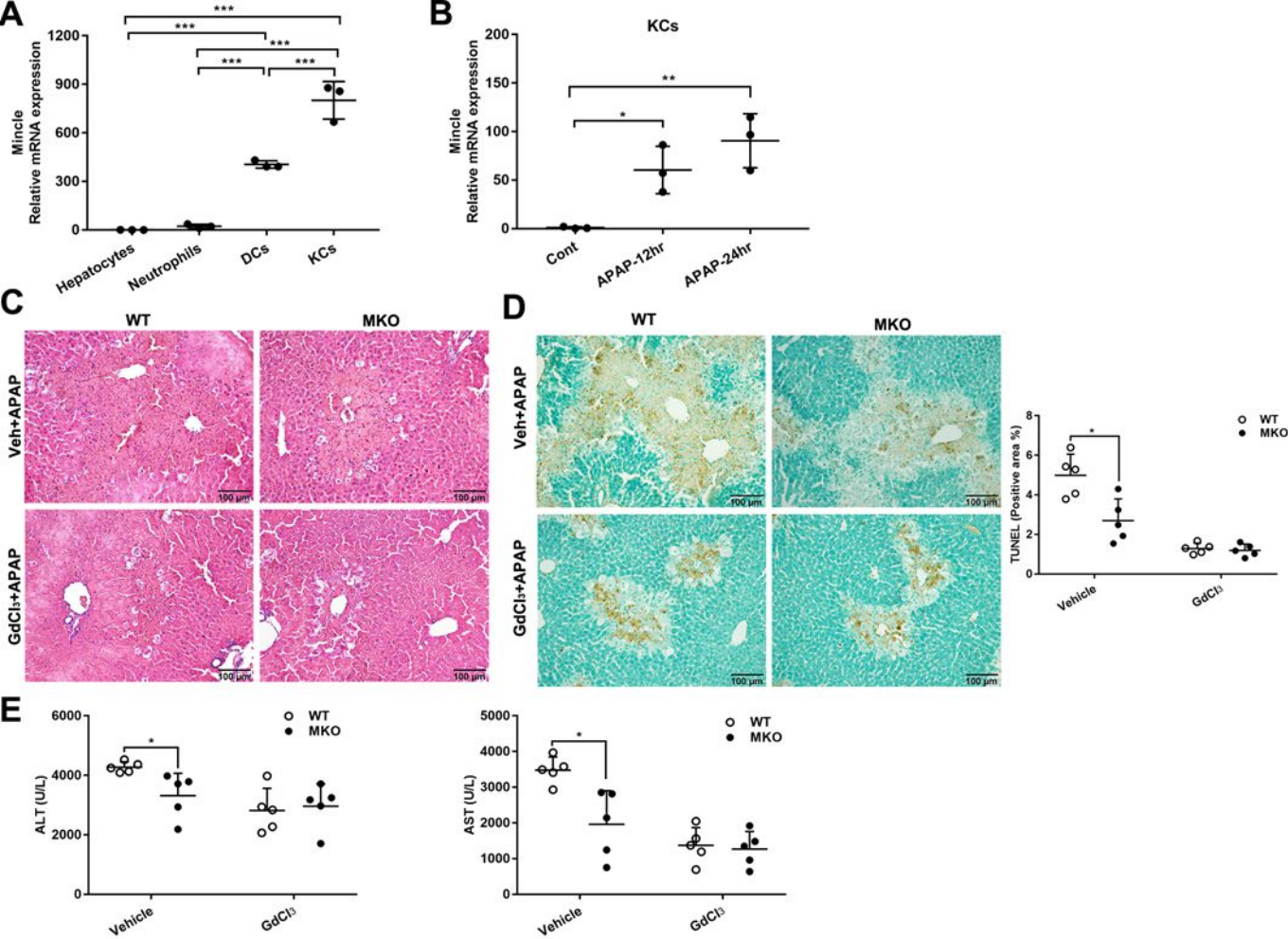


Figure 6

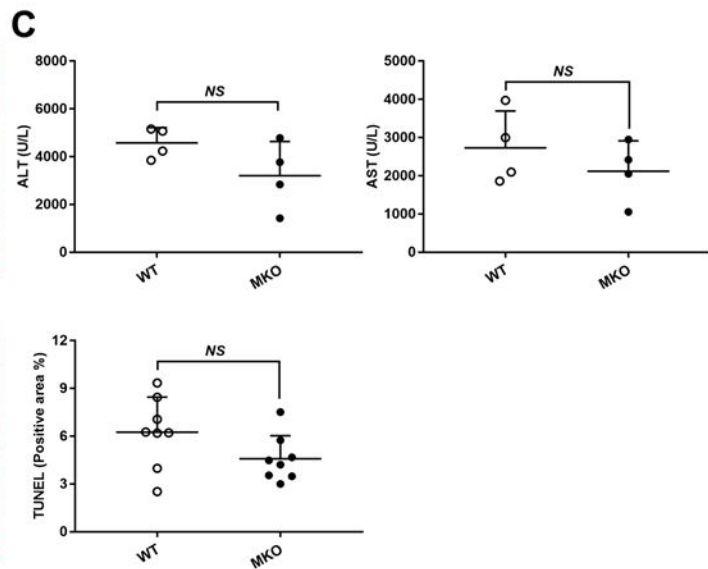
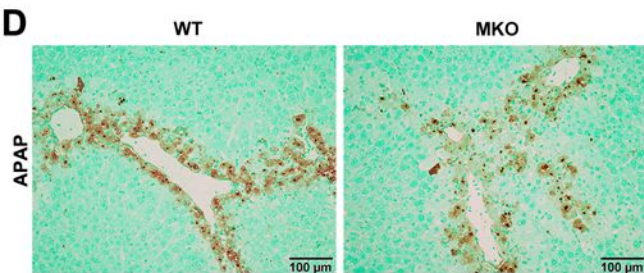
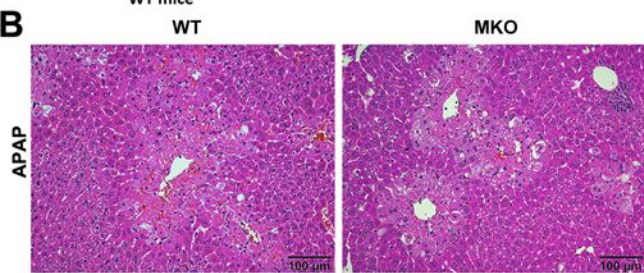
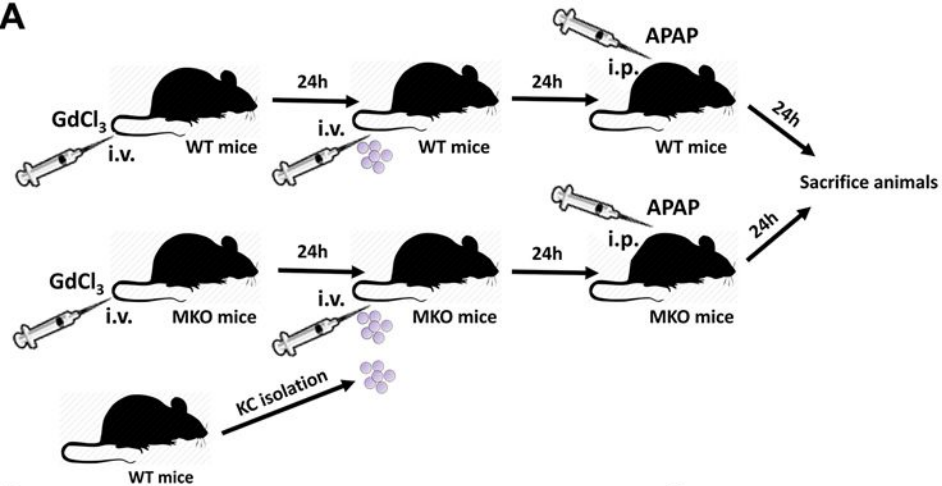


Figure 7

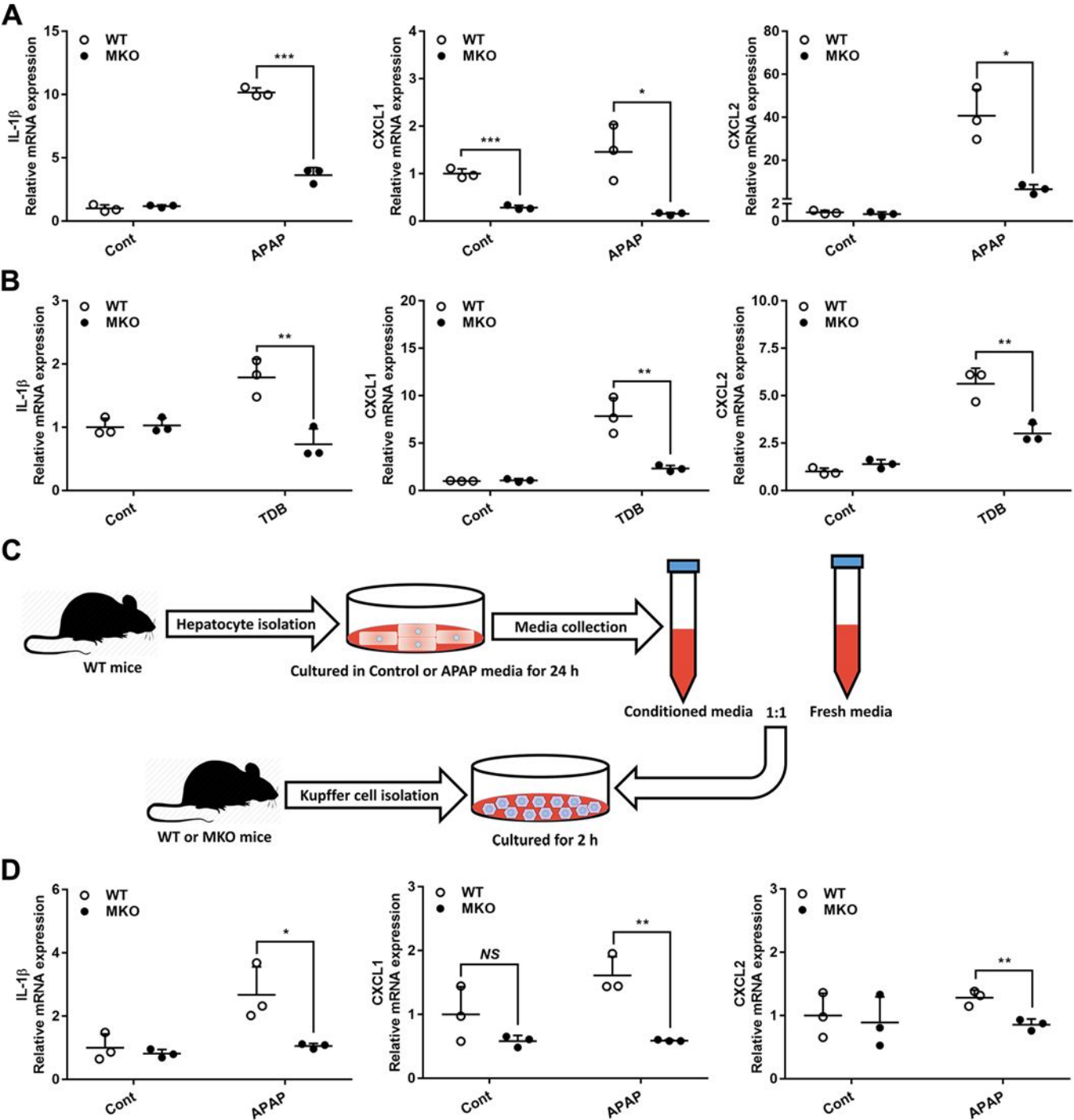


Figure 8

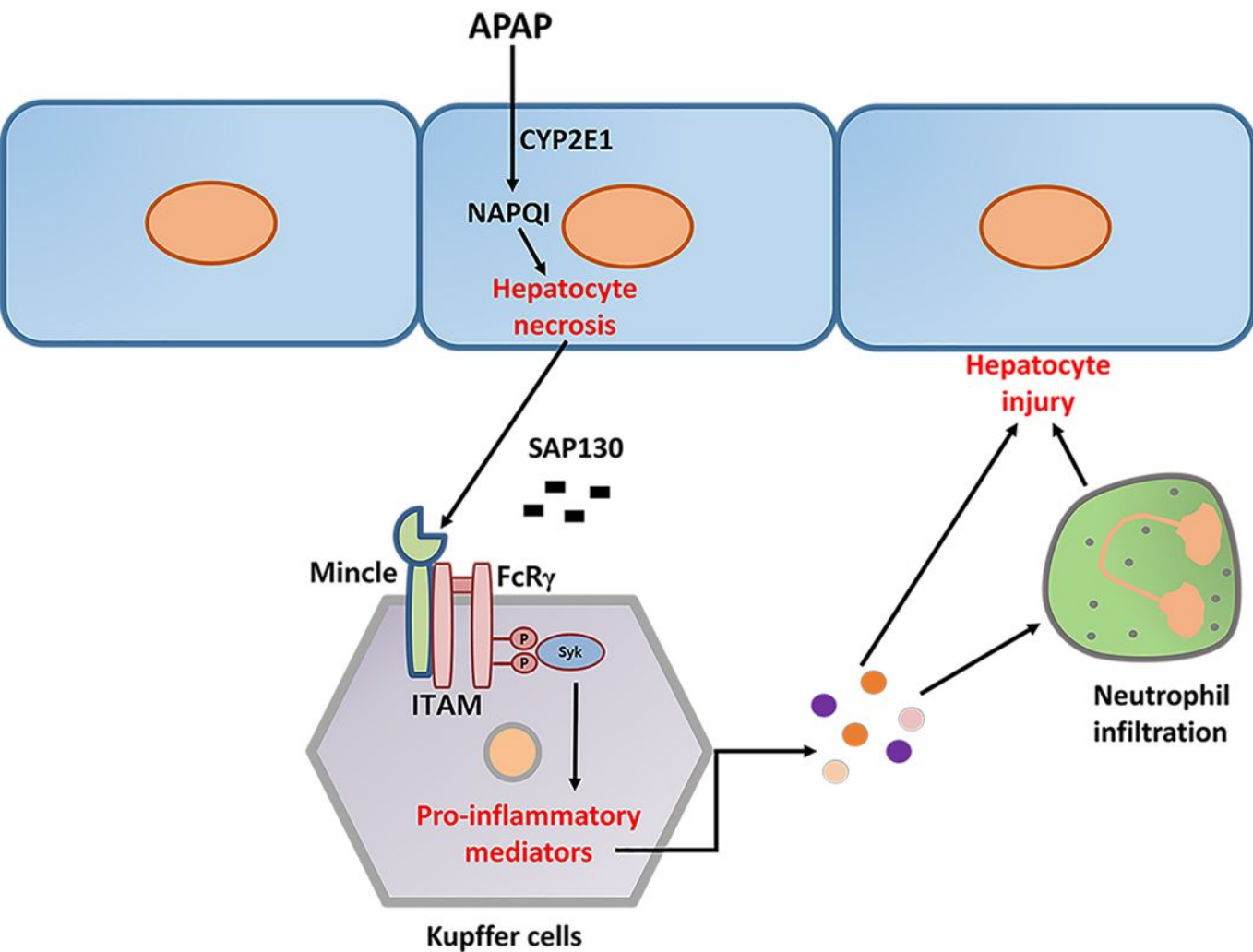


Figure 9